Influence of Rare Earth (Pr^{3+}) Dopant, on Rietveld Structure Refitment and Cation Distribution of Cobalt Ferrite, Synthesised by Sol-Gel Auto - combustion Method.

[1]A.M.Pachpinde, [2]M.M.Langade,
[1]Associate Professor, [2]Assistant Professor
[1]Department of Chemistry,
[1]Jawahar ASC College, Anadur,(M.S.) India

Abstract : Praseodymium (Pr^{3+}) substituted cobalt ferrite nanoparticles $Pr_xCoFe_{2-x}0_4$ (x = 0.000, 0.025 , 0.050 , 0.075 and 0.100) were synthesised by sol-gel auto combustion method. The precursor samples were calcinated at 600 °C , for six hours. The ferrite samples were characterised by X-ray, on Philips x-ray diffractometer, Model 3710, using Cu-Kα radiation (λ= 1.5405 A°). The lattice parameter, the mean size of nano particles, the oxygen positional parameter and cation distribution have been determined by using Rietveld analysis. Lattice constant 'a' increases from 8.373- 8.423 Å with increase in Pr^{3+} substitution. Hopping lengths L_A and L_B increases with Pr^{3+}substitution. The mean ionic radius of the tetrahedral A- and octahedral B-sites increased with an increase in Pr^{3+} substitution.

IndexTerms **- Cobalt ferrite; Rietveld analysis; cation distribution; lattice parameter.**

I. Introduction

Spinel ferrite having formula AB_2O_4, are made of about 70% iron oxide (Fe_2O_3) and about 30 % other metal oxides such as, CuO , CoO , NiO, MnO, MgO , FeO, etc. [1] From five decades these materials have been most attractive for research due to their most remarkable applications in electronics , dialectical , optical and catalytical field ,[2,3] the physical properties of ferrite sample are dependent on, method of synthesis, and distribution of cation either A or B sites , are totally dependent on their ionic radius, crystal field , ionic polarisation and electronic configuration of dopant. [4,6]

Cobalt ferrite spinel particles shown verity of novel properties like cations , their charges and their distribution amongst tetrahedral and octahedral sites, can be controlled by experimental conditions during synthesis, so different methods are used for synthesis of ferro spinel compound such as, standard ceramic method, chemical co-precipitation, thermal decomposition of oxalate, citrate, tartrate precursor, sol-gel auto-combustion method, etc, [7] among these different method, to synthesised homogeneous particles in bulk scale, co- precipitation and sol-gel method are best methods. Among both method, sol-gel method widely used because of low processing temperature and excellent chemical homogeneity in end product [8,9].

Spinel ferrite are also doped by rare earth cations such as Y^{3+}, Gd^{3+}, HO^{3+}, Nd^{3+}, Pr^{3+}, etc., its resulting mixed ferrites have natural structure , lattice strain disturbed resulting increase in electric and magnetic parameters [10,11]. In present work we report, the effect of rare earth ion dopant, Prasodymium (Pr^{3+}) in cobalt ferrite and its influence on lattice structure parameter and distribution of cation in two sublattice namely tetrahedral (A) and octa hederal [B] sites. We have successfully prepared nano spinal ferrites Pr_xCoFe_2-xO_4 (x= 0.00 to 0.1,in step of 0.025) by sol-gel auto combination, followed by heat transmit at 600 °C for six hours and are characterised x-ray diffraction with scanning rate, one degree per minute.

II. Experimental

A series of Pr^{3+} doped $CoFe_{2-x}O_4$, in step of 0.025 prepared by sol-gel auto combination method, from pure $Fe(NO_3)_3.9H_2O$ (99.9%), $Co(NO_3)_2.6H_2O$, Citric acid and Ammonia solution (Merck India), were used as starting material . Initially aqueous solution citric acid mixed with aqueous solution of metal nitrate fallowed by addition of ammonia solution till to PH ≅ 7, the solution was heated on magnetic stirrer till temperature approximately 90 °C , with continuous stirring until the gel formed, continued the heating then get spontaneously brined and it converted into fine powder. All samples were calcinated at 600°C, for six hours, the calcinated samples analysed by X-rays spectroscopy to identify structural parameters using Philips X-ray diffractometer with Cu Kα (λ = 1.5405 A°) as the radiation source. The refinement of structure was confirmed using software, Win Ploter (Version LIB.LCMS).

III. Result and Discussion

Fig. 1 shows XRD patterns of all prepared samples, were indexed and cubic lattice was observed, all materials has well defined crystalline single phase of fcc system, with few traces of secondary phases (* PrO_3). The observed diffraction peaks assigned to different planes of (111),(220), (311), (400), (422), (511), and (440) indexed to single phase, are in good arrangement with standard values given in JCPDS data (80-2377).

The X-ray diffraction patterns shows small changes in peaks position because of unstable d-spacing values with increasing Pr^{3+} content in all ferrite samples. The replacement of Fe^{3+} ions in octahedral B site by Pr^{3+} change in expansion of unit cell, resulting in increasing of lattice constant [12]. The lattice parameter 'a' was calculated using the following equation,

$$a = d\sqrt{(h^2 + k^2 + l^2)} \quad (1)$$

Where d is the inter-planer spacing and (hkl) is the index of the XRD reflection peak.

The values of lattice contestant are represented in Table1. It is observed that lattice constant 'a' increases from 8.373- 8.423 Å with increase in Pr^{3+} substitution. The ionic radius of Pr^{3+} and Fe^{3+} ions is 1.13 and 0.67 respectively, therefore, when Fe^{3+} was replaced byPr^{3+} the lattice constant should aggrandize as the content of the Pr^{3+} increased.

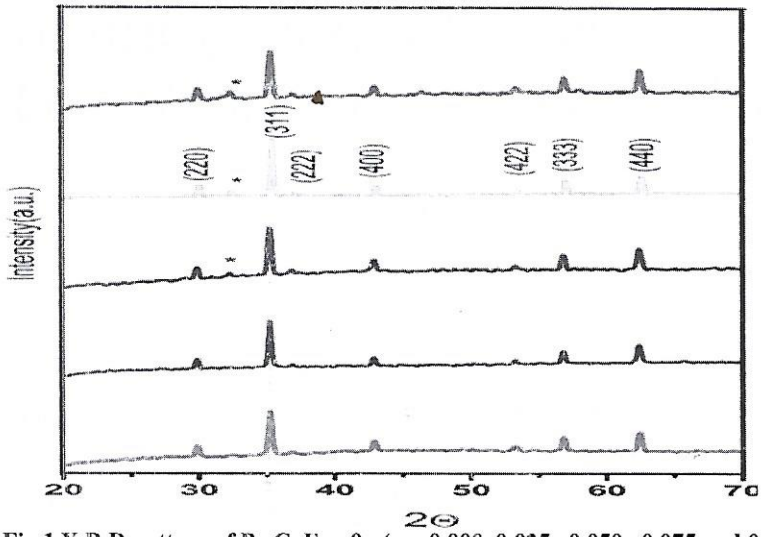

Fig.1.X.R.D.pattens of $Pr_xCoFe_{2-x}0_4$ (x = 0.000, 0.025 , 0.050 , 0.075 and 0.100)

Table 1.The value of lattice constant (a), goodness factor ($\chi 2$), discrepancy factor (Rwp), expected values(Rexp), tetrahedral and octahedral bond length (d_{AX} and d_{BX}) tetrahedral edge , shared and unshared octahedral edges (d_{AXE} , d_{BXE} and d_{BXEU})system $Pr_xCoFe_{2-x}0_4$ (x = 0.000, 0.025 , 0.050 , 0.075 and 0.100)

Comp. x	lÅ	χ^2	R_{wp}	R_{EXP}	d_{AX}	d_{BX}	d_{AXE}	d_{BXE}	d_{BXEU}
0.000	8.3732	1.741	3.256	2.178	1.8999	2.0443	3.1025	2.8183	2.9621
0.025	8.3761	1.589	4.512	2.417	1.9006	2.0450	3.1036	2.8193	2.9631
0.050	8.3835	1.963	4.1024	2.621	1.9023	2.0468	3.1063	2.8218	2.9657
0.075	8.3984	1.424	3.841	2.914	1.9056	2.0504	3.1118	2.8268	2.9710
0.100	8.4234	2.654	3.945	2.541	1.9113	2.0565	3.1211	2.8352	2.9798

The refinement of the structures was carried out with software, Win Ploter (Version LIB.LCMS), from X-ray powder diffraction data. Both octahedral and tetrahedral cation and oxygen sites are assumed to be fully occupied. Diffraction profiles were modeled by using a multiterm Simpson's rule integration of the pseudo-Voigt function. The fitting quality of the experimental data were checked by using the following parameters: the goodness of fit, x^2; that must tend to 1 and two reliability factors, Rp and Rwp (weighted differences between measured and calculated values) that must be close to or less than 10%. The refined crystallographic parameters were: the scale factor; the lattice parameter, a0; the oxygen positional parameter, u; the mean particles size and the degree of inversion, *x*.

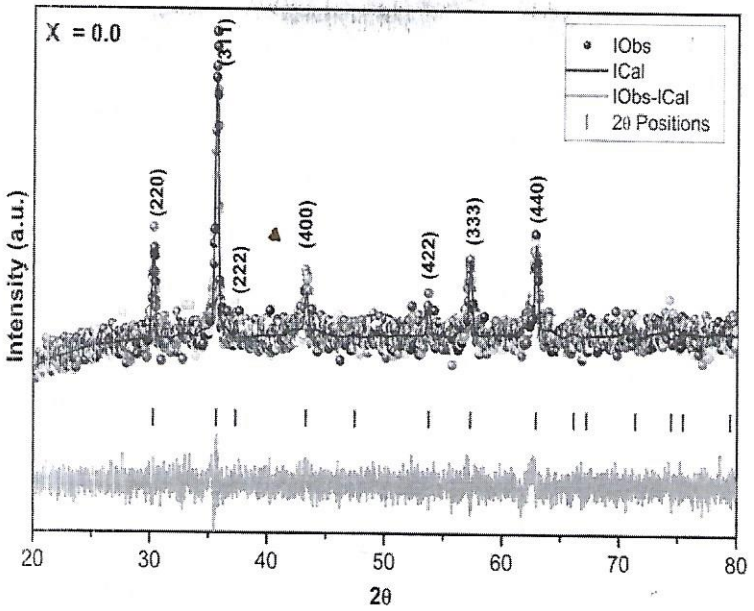

Fig 2. Typical Observed (◦) and calculated (-) X–ray diffraction pattern of $Pr_xCoFe_{2-x}0_4$ sample (x = 0.0) .

The x-ray diffraction patterns retirement was continuously done to get goodness factor near to one, the value of discrepancy factor (R_{WP}) and exapted values (R_{exp}) with goodness index are also listed in Table1. The Rietveld refined XRD patterns for typical sample x=00 of $Pr_xCoFe_{2-x}0_4$ systems is shown in the Fig. 2. Indicate observed and calculated pattern as well as their difference are much collinearly.

By using the experimental values of lattice constant, oxygen positional parameter 'u' and substituting the following equation, the allied parameters of such as tetrahedral and octahedral bond length (d_{AX} and d_{BX}) tetrahedral edge, shared and unshared octahedral edges (d_{AXE} , d_{BXE} and d_{BXEU}) were calculated by using following equations [13,15] (d_{Ax} and d_{Bx}), tetrahedral edge, shared and unshared octahedral edge (d_{AXE}, d_{BXE} and d_{BXEU}) were calculated.

$$d_{AX} = a\sqrt{3}\left(u - \frac{1}{4}\right) \quad (2)$$

$$d_{BX} = a\left[3u^2 - \left(\frac{11}{4}\right)u + \frac{43}{64}\right]^{\frac{1}{2}} \quad (3)$$

$$d_{AE} = a\sqrt{2}\left(2u - \frac{1}{2}\right) \quad (4)$$

$$d_{BEshaired} = a\sqrt{2}\left(1 - 2u\right) \quad (5)$$

$$d_{BEunshaired} = a\left(4u^2 - 3u + \frac{11}{16}\right)^{\frac{1}{2}} \quad (6)$$

Table 2. illustrates that all the allied parameter increased with the increase in Pr^{3+} substitution. The variation of allied parameters is related to the difference in the ionic radii of Pr^{3+} and Fe^{3+}. The Pr^{3+} ion with the larger ionic radii increases the allied parameter as the replaces Fe^{3+} ions of smaller ionic radii.

The hopping length for A-site (L_A) and B-sites (L_B) are calculated using the values of lattice constant.

$$L_A = a\sqrt{\frac{3}{4}} \quad (7)$$

$$L_A = a\sqrt{\frac{2}{4}} \quad (8)$$

Table 2. shows the variation of hopping lengths L_A and L_B with Pr^{3+}substitution. It is observed from Table 2. that the distance between the magnetic ions (hopping length) increases as Pr^{3+} substitution increases. This behavior of hopping lengths with Pr^{3+} substitution is an analogous with the behavior of lattice constant with Pr^{3+} substitution. This variation may be attributed to the difference in the ionic radii of the constituent ions, which makes the magnetic ions become larger to each other and the hopping length increased.

Principal
Jawahar Arts, Science & Commerce College,
Andur Tal. Tuljapur Dist. Osmanabad

Table 2. Hopping lengths(L_A and L_B), Ionic radii of tetrahedral A-site (r_A), octahedral B-site (r_B), theoretically lattice constant (a_{th}) and oxygen positional parameter (u) and Cation distribution of $Pr_xCoFe_{2-x}O_{4\,x}0_4$ (x = 0.000, 0.025 , 0.050 , 0.075 and 0.100).

Comp. x	L_A (Å)	L_B (Å)	r_A (Å)	r_B (Å)	a_{th} (Å)	u (Å)	Cation distribution
0.000	3.6257	2.9604	0.670	0.725	8.518	0.3849	$(Fe)^A\,[CoFe]^B\,O_4$
0.025	3.6270	2.9614	0.670	0.731	8.533	0.3846	$(Fe)^A\,[CoPr_{0.025}Fe_{0.975}]^B\,O_4$
0.050	3.6302	2.9640	0.676	0.734	8.550	0.3848	$(Co_{0.05}Fe_{0.95})^A\,[Co_{0.95}Pr_{0.05}Fe]^B\,O_4$
0.075	3.6366	2.9693	0.676	0.740	8.565	0.3845	$(Co_{0.05}Fe_{0.95})^A\,[Co_{0.95}Pr_{0.075}Fe_{0.975}]^B\,O_4$
0.100	3.6474	2.9781	0.681	0.743	8.582	0.3846	$(Co_{0.1}Fe_{0.9})^A\,[Co_{0.9}Pr_{0.1}Fe]^B\,O_4$

The cation distribution in spinel ferrite can be obtained from the analysis of x-ray diffraction pattern. In the present work, the Bertaut method [16] is used to determine the cation distribution. The cation distribution of $Pr_xCoFe_{2-x}O_4$ is listed in Table 4. The radius of Pr^{3+} ions was larger than that of others metal ions in the as-obtained products and the inter spaces of tetrahedral sites (A) was smaller than that of octahedral site [B], so Pr^{3+} ions was prior to occupy the octahedral sites [B].Partial migration of Co^{2+} ions (0.78Å) from B to A sites has been observed by increasing the Pr^{3+} concentration. Fe^{3+} ions showed no strong preference for any site and occupy both tetrahedral A- and octahedral B-site.

The mean ionic radius of the tetrahedral A- and octahedral B-sites (r_A and r_B) can be calculated for all the samples using the relations discussed elsewhere [17]. The values of r_A and r_B are listed in Table 2. It is observed from Table 2 that the mean ionic radius of the tetrahedral A- and octahedral B-sites increased with an increase in Pr^{3+} substitution. The increase in r_B is due to the replacement of smaller Fe^{3+} ions of ionic radii (0.67 Å) by the larger are earth Pr^{3+} ions with 1.13 Å ionic radii at octahedral B-site. The small increase in r_A is due to the migration of Co^{2+} ions from B site to A site, that resulted in the increase the octahedral radii 'r_B'.

The theoretical values of lattice parameter can be calculated with the help of following equation [18],

$$a_{th} = \frac{8}{3}\sqrt{3}\left[(r_A + R_0) + \sqrt{3}(r_B + R_0)\right] \qquad (9)$$

Where r_A and r_B are radii of tetrahedral (A) site and octahedral [B] site, R_O is radius of oxygen i.e. (R_O = 1.32 Å). The values of theoretical lattice parameter 'a_{th}' obtained by using relation (9)are shown in Table 2. It is observed that a_{th} increased from 8.518 to 8.582Å with increase in Pr^{3+} substitution. The difference between a and a_{th} may be related to the lattice defects for polycrystalline material and the presence of Fe^{3+} on A orB sites which are not taken into account [19].

Using the values of 'a', the radius of oxygen ion R_O= 1.32 Å and 'r_A' in the following expression, the oxygen positional parameter 'u' can be calculated [17],

$$u = \left[(r_A + R_0)\frac{1}{\sqrt{3}a} + \frac{1}{4}\right] \qquad (10)$$

Table 2. shows the variation of oxygen positional parameter 'u' with Pr^{3+} substitution. Our value of 'u' is larger than its ideal value (u = 0.375 Å), this larger value may probably be due to many reasons, including the history of the samples, experimental or measurement errors, e.g. precision of the observed X-ray intensity and the theoretical data used for the scattering model of the system.

IV. Conclusion

Praseodymium (Pr^{3+}) substituted cobalt ferrite nanoparticles $Pr_xCoFe_{2-x}0_4$ (x = 0.000, 0.025 , 0.050 , 0.075 and 0.100) were successfully synthesised by sol-gel auto combustion method. XRD patterns illustrates formation crystalline single phase of fcc system, with few traces of secondary phases (* PrO_3) for all samples. The Rietveld refined XRD patterns shows observed and calculated pattern are much collinearly. Lattice constant 'a' increases from 8.373- 8.423 Å with increase in Pr^{3+} substitution. All the allied parameters increased with the increase in Pr^{3+} substitution. Hopping lengths L_A and L_B increases with Pr^{3+}substitution.

The mean ionic radius of the tetrahedral A- and octahedral B-sites increased with an increase in Pr^{3+} substitution.

Principal
Jawahar Arts, Science & Commerce College,
Andur Tal. Tuljapur Dist, Osmanabad

REFERENCES

[1] Dasan, Y.K., Guan, B.H., Zahari, M.H. and Chuan, L.K., 2017. Influence of La3+ substitution on structure, morphology and magnetic properties of nanocrystalline Ni-Zn ferrite. *PloS one*, *12*(1), p.e0170075.

[2] Caizer, C. and Stefanescu, M., 2002. Magnetic characterization of nanocrystalline Ni–Zn ferrite powder prepared by the glyoxylate precursor method. *Journal of Physics D: Applied Physics*, *35*(23), p.3035.

[3] Shirsath, S.E., Toksha, B.G., Kadam, R.H., Patange, S.M., Mane, D.R., Jangam, G.S. and Ghasemi, A., 2010. Doping effect of Mn2+ on the magnetic behavior in Ni–Zn ferrite nanoparticles prepared by sol–gel auto-combustion. *Journal of Physics and Chemistry of Solids*, *71*(12), pp.1669-1675.

[4] Najmoddin, N., Beitollahi, A., Kavas, H., Mohseni, S.M., Rezaie, H., Åkerman, J. and Toprak, M.S., 2014. XRD cation distribution and magnetic properties of mesoporous Zn-substituted CuFe2O4. *Ceramics International*, *40*(2), pp.3619-3625.

[5] Ahmad, I., Abbas, T., Islam, M.U. and Maqsood, A., 2013. Study of cation distribution for Cu–Co nanoferrites synthesized by the sol–gel method. *Ceramics International*, *39*(6), pp.6735-6741.

[6] Hussain, A., Abbas, T. and Niazi, S.B., 2013. Preparation of Ni1− xMnxFe2O4 ferrites by sol–gel method and study of their cation distribution. *Ceramics International*, *39*(2), pp.1221-1225.

[7] Kurian, M., Thankachan, S., Nair, D.S., Aswathy, E.K., Babu, A., Thomas, A. and KT, B.K., 2015. Structural, magnetic, and acidic properties of cobalt ferrite nanoparticles synthesised by wet chemical methods. *Journal of Advanced Ceramics*, *4*(3), pp.199-205.

[8] Kurian, M. and Nair, D.S., 2016. Effect of preparation conditions on nickel zinc ferrite nanoparticles: a comparison between sol–gel auto combustion and co-precipitation methods. *Journal of Saudi Chemical Society*, *20*, pp.S517-S522.

[9] Rezlescu, N., Rezlescu, E., Popa, P.D., Doroftei, C. and Ignat, M., 2013. Comparative study between catalyst properties of simple spinel ferrite powders prepared by self-combustion route. *Romanian Reports in Physics*, *65*(4), pp.1348-1356

[10] Cheng, F.X., Jia, J.T., Xu, Z.G., Zhou, B., Liao, C.S., Yan, C.H., Chen, L.Y. and Zhao, H.B., 1999. Microstructure, magnetic, and magneto-optical properties of chemical synthesized Co–RE (RE= Ho, Er, Tm, Yb, Lu) ferrite nanocrystalline films. *Journal of applied physics*, *86*(5), pp.2727-2732.

[11] Kumar, B.R. and Ravinder, D., 2002. Thermoelectric power studies of gadolinium substituted Mn–Zn–Gd ferrites. *Materials Letters*, *53*(6), pp.441-445.

[12] Rezlescu, N., Rezlescu, E., Pasnicu, C. and Craus, M.L., 1994. Effects of the rare-earth ions on some properties of a nickel-zinc ferrite. *Journal of Physics: Condensed Matter*, *6*(29), p.5707.

[13] Patange, S.M., Shirsath, S.E., Jangam, G.S., Lohar, K.S., Jadhav, S.S. and Jadhav, K.M., 2011. Rietveld structure refinement, cation distribution and magnetic properties of Al3+ substituted NiFe2O4 nanoparticles. *Journal of Applied Physics*, *109*(5), p.053909..

[14] Ravinder, D., 1994. Composition dependence of the elastic moduli of mixed lithium–cadmium ferrites. *Journal of Applied Physics*, *75*(10), pp.6121-6123.

[15] Kadam, G.B., Shelke, S.B. and Jadhav, K.M., 2010. Structural and electrical properties of Sm 3+ doped Co-Zn Ferrite. *J Electron Electron Eng*, *1*, pp.15-25.

[16] Weil, L., Bertaut, F. and Bochirol, L., 1950. Propriétés magnétiques et structure de la phase quadratique du ferrite de cuivre. *Journal de Physique et le Radium*, *11*(5), pp.208-212.

[17] Standley K.J. 1972, Oxide magnetic materials, Clarendon Press, Oxford.

[18] Valenzuela, R., 2005. *Magnetic ceramics* (Vol. 4). Cambridge university press.

[19] Potakova, V.A., Zverev, N.D., and Romanov, V.P., 1972, On the cation distribution in Ni1−x−y Zny O4 spinel ferrites, Phys. Status Solidi A, 12(2), 623–627.